



# Evaluation of the mineralizing potential of the Mbengwi plutonics, Northwestern Cameroon, Central Africa

Benoît Joseph Mbassa<sup>1</sup> · Emmanuel Njonfang<sup>2</sup> · Michel Grégoire<sup>3</sup> · Zénon Itiga<sup>1</sup> · Pierre Kamgang<sup>4</sup> · Mathieu Benoit<sup>3</sup> · Paul Désiré Ndjigui<sup>4</sup> · Caroline Neh Ngwa<sup>1</sup> · Junior Désiré Nolla<sup>5</sup>

Received: 14 November 2017 / Accepted: 18 October 2018 / Published online: 30 October 2018  
© Saudi Society for Geosciences 2018

## Abstract

The Mbengwi area consists of Cenozoic alkaline rocks and Pan-African calc-alkaline plutonics. The alkaline magmatic series include volcanics (basanites, hawaiites, mugearite, and rhyolite) and syenites while the calc-alkaline plutonics comprise various granitoids (granites, granodiorites, quartz monzonites, and monzonites) associated with monzodiorites. These plutonics are calc-alkaline, metaluminous to weakly peraluminous, mostly I-type, displaying high potassic to shoshonitic affinities. Their magmas are relatively evolved and typically result from melting of the lower continental crust with variable involvement of the oceanic crust. According to the ranges of their Rb/Sr, Zr/Hf, and K/Rb ratios, these magmas have mostly not undergone post-magmatic hydrothermal activity which would lead to mineralization. With regard to their contents in certain elements such as Sr, Rb, and Ba in addition to their gradient in Sm/Eu and Rb/Ba ratios, the Mbengwi plutonics are typical of granitoids devoid of U and Ta deposits. They are also barren in Sn, W, and Mo but mostly productive regarding Cu, Zn, and Fe (Au) skarn.

**Keywords** Cameroon · Central Africa · Pan-African · Calc-alkaline plutonics · Mineralizing potential

## Introduction

Determining the mineralizing potential of intrusive bodies is important because every specific type of granite is usually accompanied with a specific type of ore deposit. Numerous precious metal deposits are spatially, temporally, and genetically associated to various types of granitic rocks (Eugster

1985; Sillitoe 1996). It had been proved that most Sn, W and several rare metal (Ta, Nb, Li, Be, Zr, Ga, REE) deposits, above 60% of Cu resources, approximately 10% of Fe, Au, Zn, Pb, Ag and U, in addition to many minor metals (Bi, Cd, Sb, Te, Re, In, Sc) are related to granitic rocks (Sillitoe 1996). Furthermore, Ghodsi et al. (2016) found that, calc-alkaline I-type magmas have a high ability to bear and concentrate base metals, notably Fe, Cu, Mo, and Au, while S-type magmas involve aqueous fluids containing Sn, W, and base metals.

Although it has been evidenced that Neoproterozoic granitoids from Cameroon host various deposits such as rare metals (Sn-W-REE; Milesi et al. 2006), very few particular attention has been focused on the geology and mineral potential of western Cameroon. Moreover, the studied area has never been so far subject of any mining exploration study. However, Mbassa (2015) revealed unusual remarkable high contents of the Mbengwi plutonics in certain elements such as Cu, Sn, Th, Pb, and Zn, which deserve a particular attention. In this paper, field works, petrographic features, and geochemical analysis are compiled to differentiate the Mbengwi Pan-African rocks either as productive or barren. We are looking forward to clarify if there may be a relationship between the geochemical composition of the studied plutonics and a possible metal mineralization. Therefore, this paper targets to

✉ Benoît Joseph Mbassa  
benjo\_mbassa@yahoo.fr

<sup>1</sup> Institute of Geological and Mining Research (IRGM), Branch for Volcanological and Geophysical Research (ARGV), P.O. Box 370, Buea, Cameroon  
<sup>2</sup> Laboratory of Geology, Higher Teacher Training College, University of Yaoundé I, P.O. Box 47, Yaoundé, Cameroon  
<sup>3</sup> Géosciences–Environnement–Toulouse, UMR 5563, Observatoire Midi Pyrénées, Université Paul-Sabatier, 14, avenue Édouard-Belin, 31400 Toulouse, France  
<sup>4</sup> Department of Earth Sciences, Faculty of Sciences, University of Yaoundé I, P.O. Box 812, Yaoundé, Cameroon  
<sup>5</sup> Institute of Geological and Mining Research, P.O. Box 4110, Yaoundé, Cameroon

evaluate the mineralizing potential of the Mbengwi plutonic rocks, in comparison with the worldwide renowned productive or sterile magmatic rocks.

## Geological setting

The Central African fold belt (CAFB; Fig. 1) known as a witness of the Pan-African orogeny in Cameroon is represented by granitic rocks and meta-volcano–sedimentary formations. This CAFB is divided into three domains: (i) the southern nappes consisting of Pan-African metamorphic units which was thrust onto the Archean Congo craton towards the south; (ii) the central area or Adamawa–Yadé domain, bounded by the Sanaga and Tcholliré–Banyo faults (Fig. 1b), consists of Neoproterozoic meta-sedimentary series and various syn- to post-kinematic calc-alkaline granitoids; (iii) the northern domain that consists of the Neoproterozoic volcano–sedimentary schists, gneisses, and orthogneisses. Overall, the granitic rocks cover a significant surface both in central and western Cameroon. They derived from different sources such as lithospheric mantle (Tchameni et al. 2006; Djouka-

Fonkwé et al. 2008), lower continental crust (Nzolang et al. 2003; Nzenti et al. 2006; Mbassa et al. 2016), or mixing between those two components (Njanko et al. 2006; Kwékam et al. 2010, 2013).

The studied zone is circumscribed between the parallels 6°06' and 5°58' North and the meridians 9°57' and 10°06' East, and lithologically marked by the presence of Pan-African plutonics, Cenozoic magmatic rocks, and sedimentary series (Fig. 1c). The Cenozoic bimodal alkaline magmatic series consist of lavas and syenites belonging to the same magmatic episode (Mbassa et al. 2012). The composition of volcanic rocks ranges from basanite to rhyolite, with a gap between 50 and 62 wt.% SiO<sub>2</sub>. Mafic lavas display OIB features and HIMU mantle isotopic signature (Mbassa et al. 2012). The Pan-African plutonics consist of monzodiorites and a continuous granitic series extending from monzonites to granites. They mostly belong to an I-type suite displaying high-potassic calc-alkaline to shoshonitic features (Mbassa et al. 2016). Actually, apart from some alluvial surveys carried out by Dumort (1968) and Peronne (1969) indicating indices of gold, rutile, iron, and manganese, no intensive prospection activity has yet been carried on the studied area.

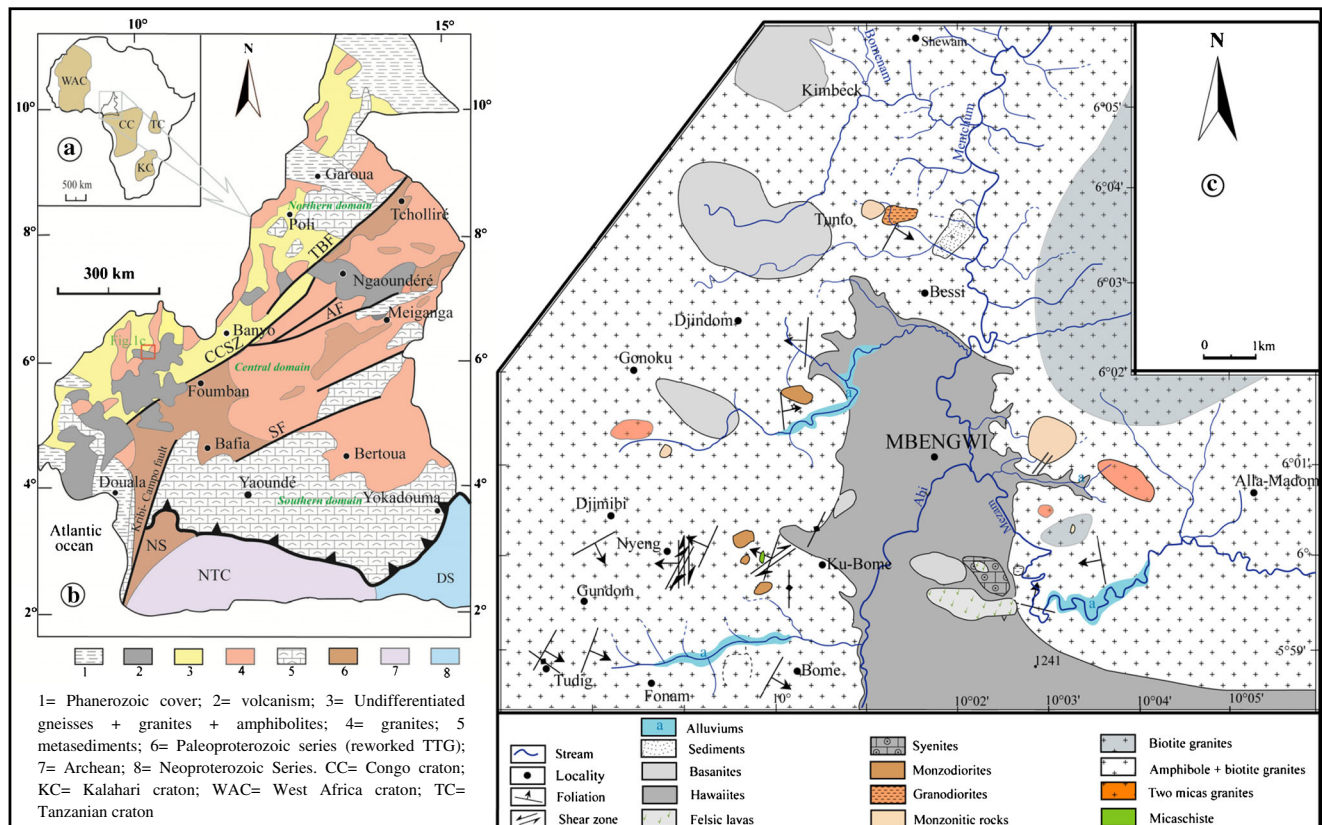


**Fig. 1** Geological setting of the studied area. **a** Location of Cameroon in Africa. **b** Simplified geological map of Cameroon showing the main Pan-African domains. AF Adamawa fault, SF Sanaga fault,

TBF: Tcholliré–Banyo fault, CCSZ: central Cameroon shear zone, NTC: Ntem complex, DS: Dja series, NS: Nyong series. **c** Geologic sketch map of the studied area

## Analytical methods

A set of 32 representative samples of Pan-African rocks from Mbengwi including granites, granodiorites, monzonites, quartz-monzonites, and monzodiorites were chosen for this study. Major elements were analyzed by ICP-OES and trace elements by ICP-MS, respectively, at the laboratories of *École des mines de Saint-Etienne* (France) and *Geosciences Environnement Toulouse* (GET-OMP, University of Toulouse 3, France). International geostandards were used. Weis and Frey (1991), Benoit et al. (1996), and Aries et al. (2000) describe analytical methods in details. The detection limits for trace elements range between  $10^{-2}$  ppm (REE) and 20 ppm (Zr).

Mineral major element compositions were determined with a CAMECA SX 50, at the service of microanalysis and microscopy of *Geosciences Environnement Toulouse* (GET-OMP, University of Toulouse 3, France). Analytical conditions were 15 kV for the acceleration tension, and the beam size was  $2 \times 2 \mu\text{m}$  under 10 or 20 nA, according to resistance of mineral to the electronic beam. Acquisition times were 10 s for the peak and 5 s on both sides of the peak, for an analyzed volume of  $5 \mu\text{m}^3$ ;  $K\alpha$  lines were used.

## Petrography and geochemistry

Plutonics from Mbengwi consist of coarse-grained granitic rocks and fine-grained monzodiorites. Granitic rocks include monzonites, quartz-monzonites, granodiorites, and granites (biotite granites, amphibole-biotite granites, and two-mica granites). The monzodiorites ( $An_{27.2-44.1}$ ) outcrop within granitoids as small subrounded or elongated enclaves. The leading mineral phase assemblage including quartz (Qtz), K-feldspar, plagioclase, amphibole, and biotite is completed by muscovite in two-mica granites. The accessory phase includes ilmenite, magnetite, sphene, apatite, and zircon. Biotite (Bt) is locally transformed to chlorite or prehnite, amphibole to chlorite, epidote or calcite, and ilmenite to goethite.

Whole rock geochemical analysis for representative plutonic samples from Mbengwi including major and trace elements are listed in Table 1. The studied calc-alkaline plutonics are mainly volcanic-related, metaluminous to weakly peraluminous (Fig. 2a) and their  $\text{SiO}_2$  contents range between 48 and 77.9 wt.%. Only one sample ( $E_{125}$ :  $A/NK = 0.98$ ) can be considered as peralkaline although it contains Mg-biotites. They are of I-type with high-K to shoshonitic affinities. However, one sample of two-mica granites has typical S-type features, suggesting either the sedimentary nature of the protolith or the assimilation of sedimentary xenoliths (Mbassa et al. 2016). The studied plutonics are strongly fractionated ( $(La/Lu)_N = 4.05-102.96$ ) and characterized by LILE and LREE enrichment compared with HFSE and HREE

respectively. They also display negative Rb, K, Sr, P, Ti, Eu, and positive Th and La anomalies (Fig. 2b, c); such features are consistent with a subduction environment.

The Sr and Nd isotopic compositions of these plutonics evidence the involvement of heterogeneous crustal materials including both the lower continental and oceanic crusts during the melting processes. The Mbengwi plutonics are then specific; since the other Pan-African high-K calc-alkaline plutons from western and central Cameroon are all melting products of the continental crust only (Mbassa et al. 2016).

## Discussion

As it has been mentioned above, Mbengwi plutonics are predominantly of I-type and coexist with small outcrops of S-type rocks. According to Nédélec and Bouchez (2011), such granitoids are known to be enriched respectively in chalcophile (Cu, Ag, Zn, Ga ...) and lithophile (Sn, W, U, Nb, Ta, Be, and Li) elements. Thus, several geochemical indicators have been used to differentiate potential productive granitoids from barren ones. The comparison of the studied plutonics contents in some elements of metallogenic interest such as Cu, Sn, Pb, Th, and Zn with their Clarke as shown in Table 2 reveals that they possess interesting chemical enrichment clues. The results are discussed below.

### Sn and W mineralization

The degree and type of differentiation and oxidation state of the magma that formed granites are important to determine the potential and type of associated mineralization (Blevin 2003). The Mbengwi plutonics have  $\text{SiO}_2$  (48.11–77.90 wt.%) and  $\text{K}_2\text{O}$  (1.65–7.21 wt.%) contents in the range of Sn- and W-related granitoids, and K/Rb ratios between 132 and 955. They are mainly moderately evolved (Fig. 3a). Highly evolved granitoids, indicators of Sn, W, U, Li, Be, and REE mineralizing potential, have K/Rb ratios under 100 (Rossi et al. 2011), and Sn-related granitic rocks are predominantly of S-type (Govett and Atherden 1988). Consequently, the predominant I-type nature of the Mbengwi granitoids and their high K/Rb ratios (132–955) do not favor high concentration of the above trace and rare earth elements. The Mbengwi plutonics display high Sr, Rb, and Ba contents in addition to Sm/Eu and Rb/Ba ratios compared to related porphyry tin deposits (data from Lehmann and Mahawat 1989; Pei and Hong 1995) (Fig. 3b), meaning that the studied plutonics might not be fertile regarding tin mineralization. Otherwise, Karimpour and Bowes (1983) used diagrams such as Rb/Sr and Ce/Yb ratios versus color index ( $[CI = (\text{SiO}_2 + \text{K}_2\text{O} + \text{Na}_2\text{O}) / (\text{MgO} + \text{CaO} + \text{FeO})]$ ) to differentiate granitoids and identify their economic potential for tin, molybdenum, or copper (Fig. 4a, b). The Mbengwi granitoids when plotted in those

**Table 1** Representative whole rock major oxides (wt.%), trace elements (ppm), and rare earth elements (ppm) for plutonic samples from the Mbengwi

|                                | Monzodiorites |       |       |       | Monzonites |       |       |       | Qtz-monzonites |       |       |       | Granodiorites |       |       |       |
|--------------------------------|---------------|-------|-------|-------|------------|-------|-------|-------|----------------|-------|-------|-------|---------------|-------|-------|-------|
|                                | E141          | E134  | E131  | E135  | E142       | E33   | E63   | E69b  | E144           | E42   | E67   | E64   | E65           | E125  | E41   | E54   |
| SiO <sub>2</sub>               | 48.81         | 48.11 | 51.44 | 54.84 | 55.58      | 50.37 | 61.92 | 60.81 | 66.90          | 63.24 | 62.11 | 67.57 | 68.07         | 69.80 | 66.64 | 64.93 |
| TiO <sub>2</sub>               | 1.47          | 1.82  | 1.41  | 1.28  | 1.15       | 1.62  | 1.48  | 0.96  | 0.99           | 1.05  | 1.47  | 0.50  | 0.46          | 0.34  | 0.67  | 0.64  |
| Al <sub>2</sub> O <sub>3</sub> | 15.37         | 17.11 | 16.74 | 16.96 | 16.33      | 19.43 | 16.15 | 14.35 | 15.79          | 15.66 | 16.10 | 15.98 | 16.13         | 14.26 | 15.69 | 17.05 |
| Fe <sub>2</sub> O <sub>3</sub> | 1.38          | 1.50  | 1.28  | 1.02  | 1.09       | 1.28  | 0.79  | 0.88  | 0.58           | 0.89  | 0.79  | 0.64  | 0.72          | 0.51  | 0.96  | 0.58  |
| FeO                            | 9.19          | 10.00 | 8.54  | 6.79  | 7.24       | 8.51  | 5.26  | 5.88  | 2.57           | 5.92  | 5.26  | 2.84  | 2.40          | 1.71  | 4.27  | 3.85  |
| MnO                            | 0.17          | 0.16  | 0.20  | 0.12  | 0.23       | 0.12  | 0.08  | 0.14  | 0.05           | 0.11  | 0.08  | 0.04  | 0.05          | 0.04  | 0.09  | 0.11  |
| MgO                            | 8.39          | 6.51  | 6.19  | 3.91  | 5.28       | 3.94  | 1.91  | 2.85  | 1.19           | 1.17  | 1.79  | 0.64  | 0.47          | 0.75  | 1.59  | 1.70  |
| CaO                            | 9.47          | 8.81  | 8.22  | 6.77  | 6.07       | 7.04  | 4.25  | 5.34  | 2.57           | 3.16  | 4.06  | 1.70  | 1.37          | 1.95  | 3.28  | 3.93  |
| Na <sub>2</sub> O              | 3.00          | 3.12  | 3.32  | 3.88  | 4.08       | 4.77  | 3.61  | 3.03  | 3.74           | 4.07  | 3.74  | 3.53  | 4.26          | 5.52  | 4.88  | 4.61  |
| K <sub>2</sub> O               | 2.22          | 2.65  | 2.34  | 3.75  | 2.55       | 2.39  | 4.12  | 5.59  | 5.28           | 4.44  | 4.18  | 6.40  | 5.96          | 5.01  | 1.65  | 2.35  |
| P <sub>2</sub> O <sub>5</sub>  | 0.53          | 0.21  | 0.31  | 0.68  | 0.40       | 0.53  | 0.42  | 0.17  | 0.35           | 0.30  | 0.43  | 0.15  | 0.11          | 0.11  | 0.28  | 0.25  |
| Total                          | 100           | 100   | 100   | 100   | 100        | 100   | 100   | 100   | 100            | 100   | 100   | 100   | 100           | 100   | 100   | 100   |
| Ag                             | <1            | <1    | <1    | <1    | <1         | <1    | <1    | <1    | <1             | <1    | <1    | <1    | <1            | <1    | <1    | <1    |
| Ba                             | 849           | 660   | 322   | 2010  | 300        | 1185  | 1540  | 473   | 1560           | 1585  | 1720  | 999   | 937           | 764   | 259   | 855   |
| Co                             | 47.3          | 46    | 42.6  | 42.5  | 38.5       | 35    | 30.2  | 28    | 47             | 38.1  | 48.5  | 39.9  | 30.9          | 44.3  | 31.2  | 38.8  |
| Cr                             | 370           | 30    | 70    | 10    | 200        | <10   | 10    | 30    | <10            | <10   | 10    | <10   | <10           | <10   | 10    | <10   |
| Cs                             | 4.54          | 4.76  | 7.14  | 1.48  | 8.25       | 3.56  | 9.55  | 1.17  | 8.12           | 11.55 | 2.82  | 6.02  | 10.15         | 4.17  | 4.53  | 2.14  |
| Cu                             | 39            | 68    | 37    | 238   | 114        | 23    | 6     | 22    | 15             | 12    | 13    | <5    | <5            | <5    | 29    | <5    |
| Ga                             | 21.7          | 21.9  | 24.4  | 22    | 31.9       | 26.5  | 24.7  | 23    | 26             | 24.9  | 25.5  | 25.2  | 25.3          | 19.6  | 26.4  | 25.5  |
| Hf                             | 2.6           | 3.1   | 2.2   | 6.4   | 13.6       | 8.3   | 9.9   | 8.1   | 8.6            | 11.3  | 10.6  | 12.3  | 15.3          | 6.7   | 6.1   | 7.1   |
| Mo                             | <2            | <2    | 2     | <2    | <2         | <2    | <2    | <2    | <2             | 2     | <2    | <2    | 2             | <2    | <2    | <2    |
| Nb                             | 11.3          | 9.9   | 15.3  | 17.2  | 27.2       | 13.1  | 25.5  | 29.8  | 29.5           | 31.2  | 25.5  | 26.1  | 15.7          | 13.3  | 11.2  | 15.8  |
| Ni                             | 93            | 28    | 35    | 13    | 67         | 15    | 8     | 19    | 5              | <5    | 6     | <5    | <5            | <5    | <5    | <5    |
| Pb                             | 14            | 11    | 13    | 25    | 16         | 13    | 23    | 25    | 32             | 29    | 24    | 29    | 28            | 27    | 18    | 25    |
| Rb                             | 120           | 126   | 154   | 104.5 | 180.5      | 114   | 182.5 | 113   | 238            | 178   | 170.5 | 156.5 | 199           | 178.5 | 91.1  | 80    |
| Sn                             | 3             | 3     | 6     | 3     | 10         | 2     | 3     | 2     | 6              | 4     | 3     | 2     | 1             | 2     | 5     | 6     |
| Sr                             | 862           | 564   | 490   | 882   | 346        | 1040  | 555   | 195.5 | 683            | 390   | 600   | 233   | 166.5         | 272   | 262   | 540   |
| Ta                             | 0.6           | 0.7   | 1.1   | 1.4   | 1          | 0.7   | 1.4   | 2     | 2.9            | 2.1   | 1.4   | 1.1   | 0.3           | 1.3   | 0.8   | 1.4   |
| Th                             | 3.67          | 3.48  | 5.72  | 12.85 | 14.55      | 3.67  | 14.3  | 17.25 | 26.2           | 12.7  | 16.05 | 26.6  | 28.9          | 44.4  | 8.99  | 36.3  |
| Tl                             | 0.5           | 0.5   | 0.6   | <0.5  | 0.6        | 0.5   | 0.8   | 0.5   | 1              | 0.7   | 0.7   | 0.7   | 0.9           | 0.7   | <0.5  | <0.5  |
| U                              | 0.66          | 1.61  | 1.77  | 4.14  | 4.64       | 0.9   | 3.68  | 3.12  | 7.96           | 4.08  | 2.41  | 2.77  | 4.39          | 2.34  | 1.8   | 5.02  |
| V                              | 246           | 349   | 246   | 189   | 138        | 204   | 72    | 96    | 57             | 44    | 72    | 18    | 9             | 33    | 76    | 66    |
| W                              | 22            | 25    | 39    | 56    | 61         | 29    | 78    | 55    | 206            | 143   | 179   | 188   | 151           | 224   | 114   | 154   |
| Zn                             | 123           | 122   | 155   | 89    | 216        | 142   | 124   | 152   | 76             | 124   | 128   | 86    | 88            | 43    | 104   | 113   |

**Table 1** (continued)

|                                |       |       |       |       |       |       |       |       |       |       |       |       |       |       |       |                         |
|--------------------------------|-------|-------|-------|-------|-------|-------|-------|-------|-------|-------|-------|-------|-------|-------|-------|-------------------------|
| Zr                             | 69    | 105   | 64    | 238   | 497   | 327   | 404   | 282   | 295   | 466   | 430   | 466   | 580   | 213   | 218   | 259                     |
| Y                              | 23.1  | 19.5  | 32.8  | 31.4  | 65.4  | 20.2  | 16.5  | 36.2  | 34    | 31.6  | 17.2  | 31.6  | 28.4  | 17.2  | 21.9  | 32.1                    |
| La                             | 34.8  | 19.4  | 28.1  | 46.9  | 38.7  | 41.9  | 149.5 | 72.7  | 82.4  | 74.1  | 100   | 166   | 130   | 45.2  | 29.9  | 62.7                    |
| Ce                             | 70.6  | 42    | 57.6  | 105   | 93.4  | 92.6  | 227   | 135   | 183.5 | 141.5 | 177   | 294   | 285   | 85.5  | 61.3  | 119.5                   |
| Pr                             | 8.16  | 5.11  | 8.1   | 12.05 | 14.1  | 11.6  | 22.3  | 15.85 | 20.3  | 15.85 | 18.45 | 29.6  | 25.3  | 8.49  | 7.11  | 12.65                   |
| Nd                             | 33.8  | 22.7  | 36.8  | 48.1  | 66.3  | 49.1  | 73.3  | 60.9  | 75.7  | 61    | 65.6  | 102   | 87.3  | 29.6  | 30.2  | 46.5                    |
| Sm                             | 6.87  | 5.09  | 8.56  | 8.86  | 16.7  | 9.3   | 9.68  | 10.85 | 12.2  | 10.5  | 9.64  | 15    | 13.5  | 5     | 7.02  | 8.67                    |
| Eu                             | 2.04  | 1.56  | 1.9   | 2.79  | 2.36  | 2.65  | 2.4   | 1.01  | 2.3   | 2.43  | 2.27  | 1.42  | 1.41  | 0.97  | 1.37  | 1.52                    |
| Gd                             | 6.46  | 4.88  | 7.76  | 7.93  | 14.4  | 7.71  | 8.51  | 9.88  | 9.74  | 9.13  | 7.74  | 13.15 | 12.15 | 4.56  | 6.34  | 7.86                    |
| Tb                             | 0.95  | 0.75  | 1.21  | 1.18  | 2.28  | 1.04  | 0.91  | 1.45  | 1.14  | 1.29  | 0.91  | 1.63  | 1.52  | 0.63  | 0.9   | 1.18                    |
| Dy                             | 4.73  | 3.95  | 6.49  | 6     | 12    | 4.7   | 3.64  | 7.29  | 5.02  | 6.27  | 3.76  | 7.16  | 6.8   | 3.24  | 4.38  | 6.24                    |
| Ho                             | 0.9   | 0.75  | 1.23  | 1.16  | 2.31  | 0.75  | 0.63  | 1.4   | 0.97  | 1.17  | 0.65  | 1.27  | 1.19  | 0.62  | 0.82  | 1.19                    |
| Er                             | 2.49  | 2.13  | 3.5   | 3.37  | 6.56  | 1.92  | 1.77  | 3.96  | 2.89  | 3.43  | 1.8   | 3.4   | 3.25  | 1.83  | 2.27  | 3.53                    |
| Tm                             | 0.31  | 0.29  | 0.49  | 0.48  | 0.94  | 0.22  | 0.2   | 0.55  | 0.37  | 0.45  | 0.21  | 0.39  | 0.37  | 0.27  | 0.32  | 0.5                     |
| Yb                             | 1.89  | 1.78  | 3.13  | 3.04  | 5.87  | 1.26  | 1.23  | 3.45  | 2.42  | 2.93  | 1.26  | 2.34  | 2.22  | 1.79  | 1.97  | 3.08                    |
| Lu                             | 0.29  | 0.26  | 0.46  | 0.5   | 0.9   | 0.18  | 0.18  | 0.53  | 0.42  | 0.45  | 0.18  | 0.34  | 0.33  | 0.27  | 0.3   | 0.44                    |
| A/NK                           | 2.95  | 2.97  | 2.95  | 2.22  | 2.46  | 2.72  | 2.09  | 1.67  | 1.75  | 1.84  | 2.03  | 1.61  | 1.58  | 1.35  | 2.40  | 2.45                    |
| A/CNK                          | 1.05  | 1.17  | 1.21  | 1.18  | 1.29  | 1.37  | 1.35  | 1.03  | 1.36  | 1.34  | 1.34  | 1.37  | 1.39  | 1.14  | 1.60  | 1.57                    |
| Sm/Eu                          | 3.37  | 3.26  | 4.51  | 3.18  | 7.08  | 3.51  | 4.03  | 10.74 | 5.30  | 4.32  | 4.25  | 10.56 | 9.57  | 5.15  | 5.12  | 5.70                    |
| Rb/Sr                          | 0.14  | 0.22  | 0.31  | 0.12  | 0.52  | 0.11  | 0.33  | 0.58  | 0.35  | 0.46  | 0.28  | 0.67  | 1.20  | 0.66  | 0.35  | 0.15                    |
| Zr/Hf                          | 26.54 | 33.87 | 29.09 | 37.19 | 36.54 | 39.40 | 40.81 | 34.81 | 34.30 | 41.24 | 40.57 | 37.89 | 37.91 | 31.79 | 35.74 | 36.48                   |
| Sr/Y                           | 37.32 | 28.92 | 14.94 | 28.09 | 5.29  | 51.49 | 33.64 | 5.40  | 20.09 | 12.34 | 34.88 | 7.64  | 5.86  | 15.81 | 11.96 | 16.82                   |
| Amph+ Bt-granite               |       |       |       |       |       |       |       |       |       |       |       |       |       |       |       |                         |
| Bt-granites                    |       |       |       |       |       |       |       |       |       |       |       |       |       |       |       |                         |
| SiO <sub>2</sub>               | E68   | E69   | E611  | R2    | E2    | E6    | E12   | E20   | E53   | E126  | E129  | E145  | E610  | E60   | E62   | Leucocratic granite E66 |
| TiO <sub>2</sub>               | 71.42 | 71.57 | 72.46 | 72.67 | 71.81 | 70.83 | 75.36 | 77.51 | 77.24 | 72.93 | 71.60 | 72.36 | 74.06 | 69.65 | 74.32 | 77.90                   |
| Al <sub>2</sub> O <sub>3</sub> | 0.35  | 0.38  | 0.38  | 0.26  | 0.33  | 0.46  | 0.36  | 0.09  | 0.15  | 0.28  | 0.23  | 0.48  | 0.18  | 0.43  | 0.08  | 0.03                    |
| Fe <sub>2</sub> O <sub>3</sub> | 13.74 | 13.77 | 14.48 | 14.25 | 14.24 | 14.78 | 12.13 | 12.95 | 12.50 | 14.08 | 14.72 | 13.84 | 14.36 | 15.45 | 14.46 | 12.36                   |
| FeO                            | 0.81  | 0.79  | 0.46  | 0.35  | 0.50  | 0.42  | 0.50  | 0.13  | 0.15  | 0.42  | 0.48  | 0.59  | 0.46  | 0.50  | 0.19  | 0.05                    |
| FeO                            | 2.69  | 2.62  | 1.54  | 1.17  | 1.67  | 1.41  | 1.65  | 0.45  | 0.49  | 1.39  | 1.60  | 1.96  | 1.53  | 2.24  | 0.62  | 0.17                    |
| MnO                            | 0.06  | 0.07  | 0.07  | 0.04  | 0.05  | 0.03  | 0.04  | 0.01  | 0.01  | 0.03  | 0.03  | 0.03  | 0.06  | 0.04  | 0.03  | 0.00                    |
| MgO                            | 0.26  | 0.23  | 0.13  | 0.39  | 0.66  | 0.56  | 0.22  | 0.16  | 0.17  | 0.50  | 0.56  | 0.88  | 0.27  | 0.69  | 0.20  | 0.06                    |
| CaO                            | 1.00  | 0.85  | 0.97  | 1.24  | 1.35  | 1.47  | 0.39  | 1.63  | 0.78  | 1.42  | 1.29  | 2.04  | 0.54  | 1.65  | 0.98  | 0.39                    |
| Na <sub>2</sub> O              | 3.93  | 3.70  | 3.36  | 3.58  | 3.10  | 4.32  | 2.21  | 3.98  | 3.02  | 3.09  | 3.20  | 3.38  | 3.13  | 3.62  | 4.16  | 2.71                    |
| K <sub>2</sub> O               | 5.68  | 5.97  | 6.16  | 5.95  | 6.18  | 5.57  | 7.12  | 3.04  | 5.45  | 5.78  | 6.22  | 4.29  | 5.41  | 5.59  | 4.89  | 6.30                    |
| P <sub>2</sub> O <sub>5</sub>  | 0.06  | 0.05  | 0.00  | 0.09  | 0.11  | 0.14  | 0.02  | 0.02  | 0.02  | 0.08  | 0.08  | 0.15  | 0.00  | 0.14  | 0.07  | 0.02                    |
| Total                          | 100   | 100   | 100   | 100   | 100   | 100   | 100   | 100   | 100   | 100   | 100   | 100   | 100   | 100   | 100   | 100                     |
| Ag                             | <1    | <1    | <1    | <1    | <1    | <1    | <1    | <1    | <1    | <1    | <1    | <1    | <1    | <1    | <1    | <1                      |
| Ba                             | 319   | 293   | 233   | 1735  | 903   | 1220  | 953   | 313   | 1195  | 1160  | 1175  | 1220  | 203   | 1275  | 797   | 700                     |
| Co                             | 52    | 56.8  | 36.5  | 50.5  | 53.1  | 51    | 57.1  | 62.1  | 79.3  | 55.2  | 47.7  | 57.8  | 46.7  | 44.7  | 55    | 81.2                    |
| Cr                             | <10   | <10   | <10   | <10   | <10   | <10   | <10   | <10   | <10   | <10   | <10   | 10    | <10   | <10   | <10   | <10                     |
| Cs                             | 1.7   | 1.53  | 0.58  | 2.54  | 4.52  | 3.44  | 4.04  | 2.54  | 1.81  | 4.06  | 3.31  | 9.07  | 10.2  | 3.02  | 5.46  | 3.42                    |
| Cu                             | <5    | 6     | <5    | <5    | 10    | <5    | <5    | <5    | 5     | <5    | 5     | <5    | <5    | <5    | <5    | 5                       |
| Ga                             | 25.4  | 24.1  | 23.1  | 19.3  | 19.4  | 21.2  | 17.3  | 17.5  | 14.6  | 19.9  | 20.1  | 23    | 26.6  | 23.6  | 22.2  | 22.5                    |
| Hf                             | 15.5  | 16.5  | 18.3  | 5.8   | 5.7   | 8.2   | 12.1  | 2.7   | 2.7   | 5.7   | 11.6  | 6.5   | 2.7   | 7.7   | 2.4   | 11.3                    |
| Mo                             | <2    | <2    | 2     | <2    | <2    | <2    | <2    | <2    | <2    | <2    | <2    | <2    | <2    | <2    | <2    | <2                      |

Table 1 (continued)

|       |       |       |       |       |       |       |       |       |       |       |       |       |       |       |       |        |
|-------|-------|-------|-------|-------|-------|-------|-------|-------|-------|-------|-------|-------|-------|-------|-------|--------|
| Nb    | 28.3  | 30.3  | 27.4  | 11.2  | 7.6   | 13.6  | 17.1  | 4     | 5.4   | 10    | 6.5   | 13.3  | 33.7  | 10.6  | 12.7  | 3.3    |
| Ni    | <5    | <5    | <5    | <5    | 5     | <5    | <5    | 8     | <5    | <5    | <5    | <5    | <5    | <5    | <5    | <5     |
| Pb    | 26    | 25    | 19    | 30    | 32    | 33    | 40    | 22    | 30    | 32    | 35    | 23    | 39    | 33    | 42    | 47     |
| Rb    | 119.5 | 113.5 | 64.5  | 170.5 | 206   | 155.5 | 219   | 86.8  | 142   | 194.5 | 187.5 | 188.5 | 230   | 151   | 170   | 170.5  |
| Sn    | 2     | 1     | 1     | 1     | 2     | 3     | 4     | 1     | 2     | 2     | 1     | 3     | 10    | 3     | 4     | <1     |
| Sr    | 78.9  | 71.2  | 62.7  | 482   | 314   | 341   | 178.5 | 217   | 368   | 366   | 389   | 706   | 73.3  | 312   | 177   | 398    |
| Ta    | 1.4   | 1.5   | 1.1   | 1     | 0.6   | 0.9   | 2     | 0.8   | 0.6   | 1.3   | 0.7   | 1.4   | 3.5   | 0.6   | 1.3   | 0.2    |
| Th    | 37.6  | 34.4  | 41.5  | 30.1  | 16.55 | 18.4  | 23.7  | 8.19  | 34.5  | 44.8  | 126   | 30    | 13.4  | 17.1  | 8.59  | 24     |
| Tl    | 0.5   | 0.5   | <0.5  | 0.6   | 0.8   | 0.7   | 0.9   | <0.5  | 0.9   | 0.9   | 0.8   | 0.7   | 1     | 0.7   | 0.9   | 0.6    |
| U     | 2.73  | 2.22  | 1.31  | 5.08  | 1.34  | 2.02  | 2.83  | 1.19  | 3.05  | 2.23  | 5.75  | 6.05  | 2.6   | 1.86  | 3.96  | 2.59   |
| V     | 8     | 6     | <5    | 19    | 23    | 9     | 11    | 5     | 13    | 23    | 36    | 40    | <5    | 18    | <5    | <5     |
| W     | 269   | 292   | 190   | 259   | 256   | 252   | 297   | 328   | 419   | 278   | 234   | 285   | 246   | 217   | 294   | 433    |
| Zn    | 95    | 88    | 71    | 30    | 64    | 43    | 42    | 16    | 15    | 42    | 36    | 70    | 102   | 63    | 43    | <5     |
| Zr    | 648   | 681   | 809   | 194   | 191   | 303   | 408   | 73    | 83    | 186   | 350   | 219   | 59    | 291   | 59    | 250    |
| Y     | 31.6  | 28.3  | 18.6  | 10.9  | 51.5  | 10.8  | 103   | 9.5   | 9.8   | 15.3  | 9.2   | 11.4  | 19.2  | 16.1  | 14.7  | 3.4    |
| La    | 284   | 242   | 367   | 79.1  | 75    | 110   | 55.6  | 20.6  | 122   | 100.5 | 110.5 | 77.8  | 29.3  | 114   | 19.9  | 9.7    |
| Ce    | 406   | 402   | 661   | 147.5 | 101   | 177.5 | 96.2  | 18.3  | 189.5 | 156.5 | 258   | 126   | 54.2  | 183   | 37.7  | 13.3   |
| Pr    | 50.4  | 43    | 66.4  | 14.55 | 12.1  | 16.35 | 14.4  | 2.73  | 16.45 | 17.3  | 22.4  | 11.5  | 6.37  | 18.75 | 4.16  | 1.12   |
| Nd    | 176.5 | 151.5 | 232   | 50    | 42.2  | 51.8  | 65.2  | 9.5   | 50.8  | 57.7  | 73.4  | 37.9  | 24.1  | 63.6  | 15.5  | 3.6    |
| Sm    | 21.1  | 18.95 | 25.4  | 7.1   | 5.98  | 6.24  | 17.8  | 1.52  | 5.91  | 7.91  | 9.74  | 5.55  | 5.43  | 8.76  | 3.38  | 0.76   |
| Eu    | 0.78  | 0.63  | 0.61  | 1.37  | 1.13  | 1.08  | 2.68  | 0.64  | 0.88  | 1.18  | 1.17  | 1.16  | 0.38  | 1.32  | 0.68  | 0.11   |
| Gd    | 16.9  | 16    | 19.7  | 5.52  | 6.26  | 5.18  | 21.8  | 1.64  | 5.2   | 6.48  | 7.26  | 4.78  | 5.02  | 7.75  | 3.22  | 0.7    |
| Tb    | 1.76  | 1.67  | 1.73  | 0.57  | 0.82  | 0.54  | 4     | 0.24  | 0.52  | 0.74  | 0.67  | 0.55  | 0.75  | 0.85  | 0.49  | 0.12   |
| Dy    | 6.78  | 6.75  | 5.41  | 2.32  | 4.65  | 2.16  | 23.4  | 1.17  | 2     | 3.12  | 2.27  | 2.36  | 3.85  | 3.48  | 2.59  | 0.68   |
| Ho    | 1.22  | 1.15  | 0.87  | 0.43  | 1.15  | 0.39  | 4.55  | 0.25  | 0.36  | 0.57  | 0.38  | 0.42  | 0.69  | 0.59  | 0.48  | 0.15   |
| Er    | 3.67  | 3.47  | 2.72  | 1.26  | 3.79  | 1.21  | 11.65 | 0.79  | 1.07  | 1.71  | 1.18  | 1.19  | 1.86  | 1.63  | 1.37  | 0.46   |
| Tm    | 0.46  | 0.42  | 0.28  | 0.17  | 0.5   | 0.15  | 1.43  | 0.12  | 0.14  | 0.23  | 0.14  | 0.15  | 0.25  | 0.17  | 0.16  | 0.09   |
| Yb    | 2.92  | 2.75  | 2.05  | 1.07  | 2.78  | 1.06  | 7.64  | 0.89  | 0.93  | 1.48  | 1.04  | 1.08  | 1.53  | 1.09  | 1.02  | 0.5    |
| Lu    | 0.51  | 0.45  | 0.37  | 0.17  | 0.49  | 0.17  | 0.92  | 0.15  | 0.13  | 0.21  | 0.17  | 0.15  | 0.23  | 0.17  | 0.15  | 0.09   |
| A/NK  | 1.43  | 1.42  | 1.52  | 1.49  | 1.54  | 1.50  | 1.30  | 1.84  | 1.48  | 1.59  | 1.56  | 1.81  | 1.68  | 1.68  | 1.60  | 1.37   |
| A/CNK | 1.30  | 1.31  | 1.38  | 1.32  | 1.34  | 1.30  | 1.25  | 1.50  | 1.35  | 1.37  | 1.38  | 1.43  | 1.58  | 1.42  | 1.44  | 1.31   |
| Sm/Eu | 27.05 | 30.08 | 41.64 | 5.18  | 5.29  | 5.78  | 6.64  | 2.38  | 6.72  | 6.70  | 8.32  | 4.78  | 14.29 | 6.64  | 4.97  | 6.91   |
| Rb/Sr | 1.51  | 1.59  | 1.03  | 0.35  | 0.66  | 0.46  | 1.23  | 0.40  | 0.39  | 0.53  | 0.48  | 0.27  | 3.14  | 0.48  | 0.96  | 0.43   |
| Zr/Hf | 41.81 | 41.27 | 44.21 | 33.45 | 33.51 | 36.95 | 33.72 | 27.04 | 30.74 | 32.63 | 30.17 | 33.69 | 21.85 | 37.79 | 24.58 | 22.12  |
| Sr/Y  | 2.50  | 2.52  | 3.37  | 44.22 | 6.10  | 31.57 | 1.73  | 22.84 | 37.55 | 23.92 | 42.28 | 61.93 | 3.82  | 19.38 | 12.04 | 117.06 |

diagrams indicate that they remain unproductive in Sn and Mo, and rather fertile regarding Cu. Elsewhere, special minerals such as tourmaline and topaz are known to be symptomatic of tin (Sn) mineralization (Rozendaal and Bruwer 1995); therefore, the non-appearance of tourmaline and topaz in the studied rocks evidences that the mineralization of tin is unlikely. The high Sn content of some granites may be justified by the fact that as Sn is hosted by muscovite, its content will increase proportionally with the amount of muscovite during differentiation process (Neiva et al. 2002). Generally, granitic rocks hosting Sn, U, and W mineralization commonly have high phosphorus concentration (Ruiz et al. 2008). Furthermore, Bea et al. (1992) specified that  $P_2O_5$  contents greater than 0.5 wt.% in rocks having more than 70 wt.%  $SiO_2$  are good indicators of economic mineralization. Taking into consideration this last statement, we realize that in Mbengwi, only granites have  $SiO_2$  contents greater than 70 wt.% and their average  $P_2O_5$  content is somewhat less than 0.5 wt.%.

### Zn mineralization

Wolfe (1977) and Lentz (1998) established a relation between the  $SiO_2$  content and the amount of Zn in granitoids. Zn amount is fixed ( $\approx 85$  ppm) for intermediate rocks, decreases linearly with increasing  $SiO_2$  in rocks having more than 60 wt.%  $SiO_2$  and reaches 35 ppm in rocks with 75 wt.%  $SiO_2$ . Almost all the studied rocks except the leucocratic granite (E<sub>66</sub>) contain Zn with amount ranging from 15 to 216 ppm. On the other hand, Wolfe (1977) stated that all rocks containing more than 10 wt.% of total iron may be good targets in regional explorations of zinc, and therefore suggested the use of  $SiO_2$  vs. Fe and  $SiO_2$  vs. Zn discriminating diagrams to decipher the sterile or fertile nature of plutonics regarding Zn detection. These diagrams disclose that the Mbengwi granitic rock samples are mostly fertile with regard to zinc (Fig. 5a, b). In mineralogy, despite the non-occurrence in the studied area of Zn-bearing mineral such as sphalerite known as major ore for Zn, the fertile character of the Mbengwi

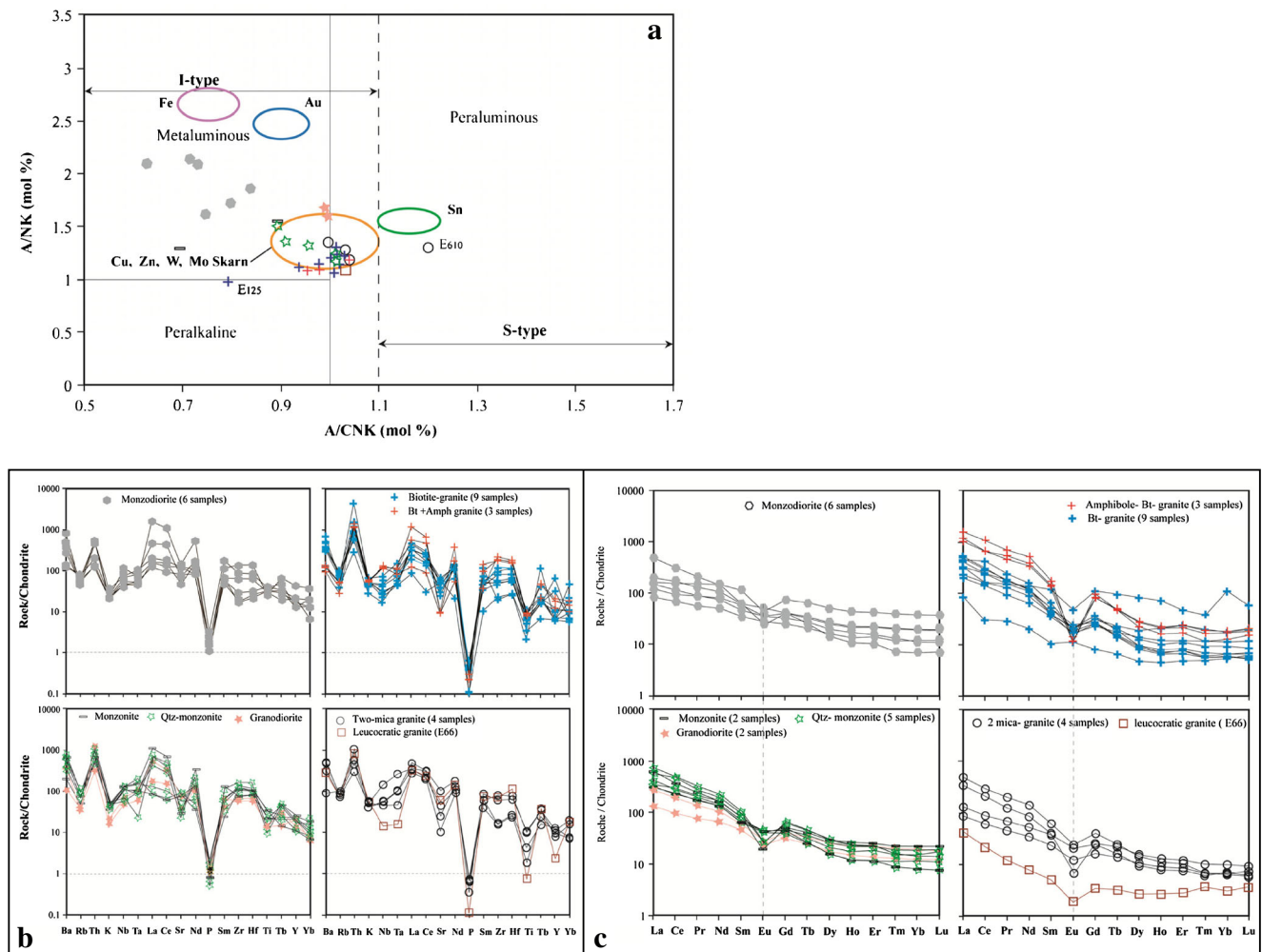


**Fig. 2** a A/NK vs. A/CNK variation diagram of Maniar and Piccoli (1989) showing the mean composition of the Mbengwi plutonic rocks with related metals. The open circles with respective names are from

Meinert (1995). b Chondrite-normalized multi-element diagrams. c Chondrite normalized rare earth element diagrams for the studied rocks. Normalization value after McDonough and Sun (1995)

**Table 2** Comparison of contents of some elements from the Mbengwi plutonics with respect to their Clarke. The Clarke are from Wedepohl (1995)

| Element | Amount within the continental crust (ppm) | Amount in the Mbengwi plutonics (ppm)         | Enriched rocks  | Rate of enrichment |
|---------|---|---|---|--------------------|
| Cu      | 25  | < 5–238 (E <sub>135</sub> )                   | Monzodiorites (E <sub>134</sub> , E <sub>135</sub> , E <sub>142</sub> )   | 2–9 times          |
| Sn      | 2   | < 1–10 (E <sub>142</sub> , E <sub>610</sub> ) | Monzodiorites (E <sub>131</sub> , E <sub>142</sub> ).<br>Quartz monzonites (E <sub>42</sub> , E <sub>144</sub> ).<br>Granodiorites. Bt-granite (E <sub>12</sub> ).<br>Two-mica granites (E <sub>62</sub> , E <sub>610</sub> ) | 2–5 times          |
| Pb      | 15  | 11–47(E <sub>66</sub> )                       | Almost all Bt-granites. Two-mica granites and leucocratic granite   | 2–3 times          |
| Th      | 9   | 3.48–126 (E <sub>129</sub> )                  | Quartz monzonites except E <sub>42</sub> .<br>Granodiorite (E <sub>54</sub> ).<br>Amph+Bt-granites. Almost all biotite-granites two-mica granite (E <sub>145</sub> )  | 2–14 times         |
| Zn      | 65  | < 5–216 (E <sub>142</sub> )                   | Almost all monzodiorite except E <sub>135</sub> .<br>All monzonites and some quartz monzonites (E <sub>42</sub> , E <sub>67</sub> )   | 2–3 times          |

granitoids regarding Zn is expressed by a significant occurrence of this metal in some biotites, magnetites, chlorites, and calcites. Chlorites and biotites hosting the highest amounts of ZnO (> 0.3 wt.%) are respectively ripidolite and Fe- or Mg-biotites. Those minerals displaying the highest amount of ZnO mostly occur in quartz monzonites (E<sub>144</sub>, E<sub>64</sub>), granodiorites (E<sub>41</sub>, E<sub>54</sub>), and in a two-mica granite (E<sub>60</sub>). The estimation of the proximity of unusual Zn concentration and accordingly potential Zn mineralization at surface in semi-arid environments can be made possible using an index based on Zn/Mn ratios in Fe–Mn crusts of Spinks et al. (2017). According to this index, values of Zn/Mn ratios above 0.006 are indicative of the proximity of a probable metal source. Apart from the leucocratic sample (E<sub>66</sub>) containing no Mn, all the studied samples have Zn/Mn ratios (0.072–0.226) higher than  $6 \times 10^{-3}$ ; therefore, samples which are assigned fertile would be mineralized very close to the surface.

### Cu mineralization

Copper and zinc behave differently during fractional crystallization process, although their chemical properties are close. Copper is mostly founded in chalcopyrite while zinc substitutes iron in ferromagnesian silicates (Bahajroy and Taki 2014). Usually, copper mineralization are found either above subduction zones in magmatic arcs or in post-collisional settings developed at the end of the subduction (Sillitoe 2010; Richards 2011). In both environments, the discrimination between the productive and the barren rocks regarding copper is routinely based on whole rock geochemistry (Baldwin and Pearce 1982; Asadi et al. 2014; Zarasvandi et al. 2015). The ore-forming granitoids display Sr/Y ratio values higher than 35, low HFSE contents, and absence of pronounced negative Eu anomalies (Shafiei et al. 2009; Hou et al. 2011; Richards et al. 2012;

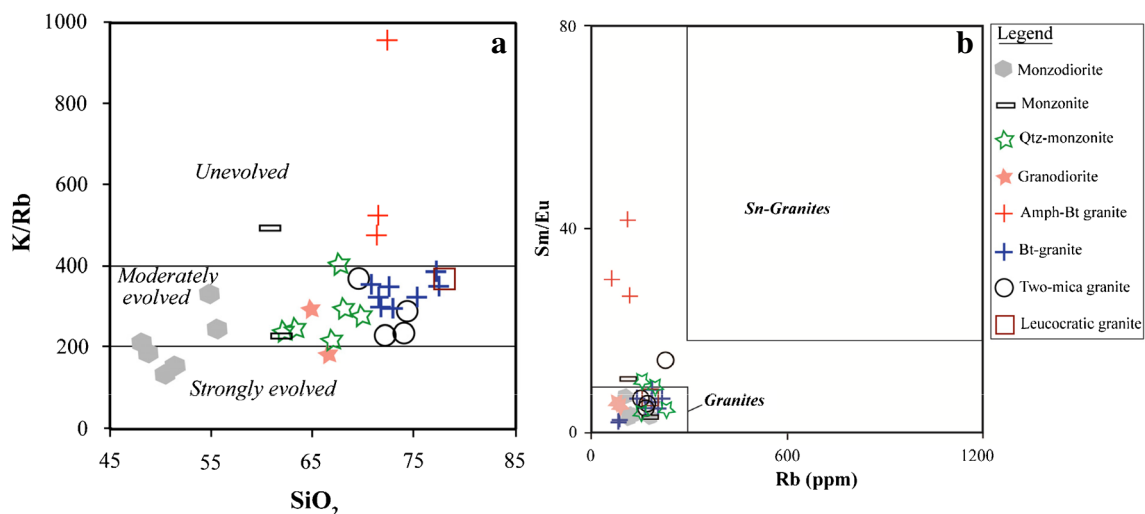


**Fig. 3** **a** Plot of K/Rb vs. SiO<sub>2</sub> (wt.%) (Blevin 2003). Most studied samples are semi-evolved. **b** Sm/Eu vs. Rb (ppm) diagram discriminating tin-bearing granites from barren ones (Karimpour and Bowes 1983)



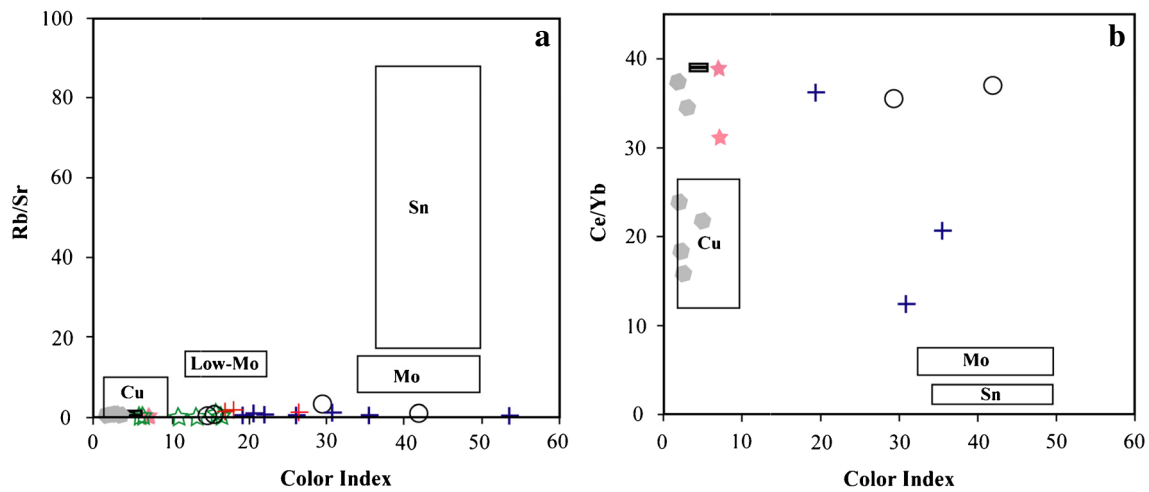


**Fig. 4** Discrimination of source rock diagrams of Cu, Sn, and Mo porphyry deposits using a color index and ratios of **a** Rb/Sr and **b** Ce/Yb (Karimpour 1999) and a plot of the study area's samples

Gao et al. 2013; Ahmadian et al. 2015; Wu et al. 2016). The Mbengwi syn- to post-collisional plutonics mainly display lower Sr/Y ratios (with very few samples having Sr/Y > 3, low HFSE contents (Table 1), and overall negative anomaly in Eu).

The use of Sr/Y vs. SiO<sub>2</sub> and Al<sub>2</sub>O<sub>3</sub>/TiO<sub>2</sub> vs. SiO<sub>2</sub> discriminating diagrams of Loucks (2014) (Fig. 6a, b) reveals that the composition of the Mbengwi plutonics overlaps both barren and productive areas. As shown in Fig. 6a, some granite samples (Bt-granite, two-mica granite, and leucocratic granite) are fertile while other plutonics are unproductive. The majority of samples are relatively barren regarding Cu deposits (Fig. 6b).

The Y versus MnO diagram of Baldwin and Pearce (1982) points out that the Mbengwi plutonics vary from barren to sub-productive and very few fertile granitoids (Fig. 7). Another discriminating diagram (Fig. 2a) also shows a productive nature for the Mbengwi calc-alkaline I-type granitoids regarding Cu and skarn ore deposits.

In order to identify if the magma could release or not hydrothermal phase, Bea et al. (2006) used Zr/Hf ratio as index; when Zr/Hf < 20, magmatic hydrothermal alteration occurred and mineralization processes are favored, and once Zr/Hf > 20, this suggests that there was no hydrothermal alteration. The Mbengwi plutonics Zr/Hf ratio ranges from 21.85 to 44.21, meaning that they have not undergone magmatic hydrothermal alteration. Although some of the previous diagrams evidenced the productive character of the Mbengwi granitoids, their overall negative Eu anomaly (Fig. 2c) is symptomatic of their low potential to be hosting massive Cu deposits.

**Skarn mineralization**

Generally, skarn mineralizations are often associated either with metaluminous to slightly peraluminous rocks or with calc-alkaline granitoids (Meinert 1995) as shown in Figs. 2a

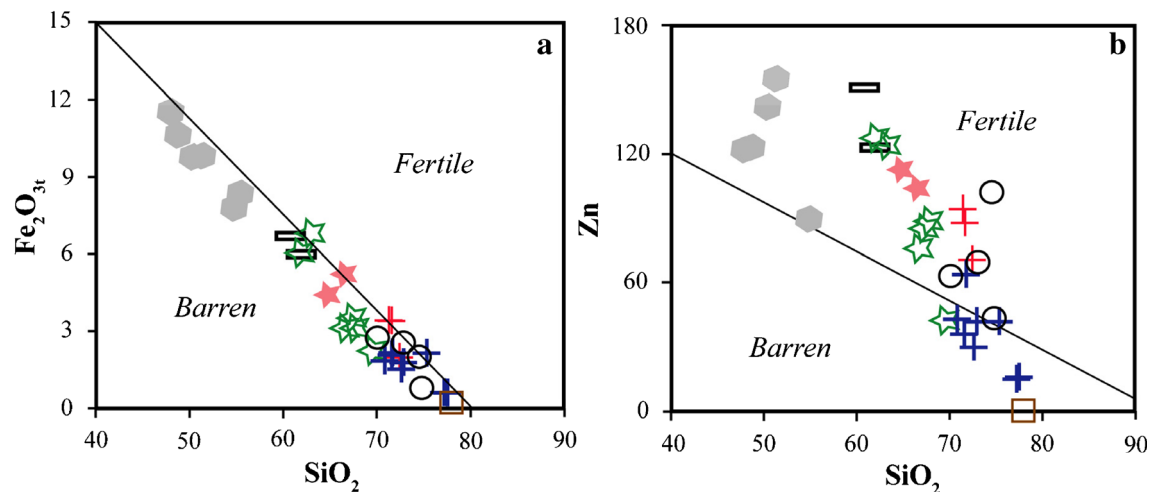


**Fig. 5** Representation of the composition of Mbengwi granitoids in **a** Fe<sub>2</sub>O<sub>3t</sub> (wt.%) and **b** Zn (ppm) vs. SiO<sub>2</sub> (wt.%) of Wolfe (1977) discriminating barren and fertile granites

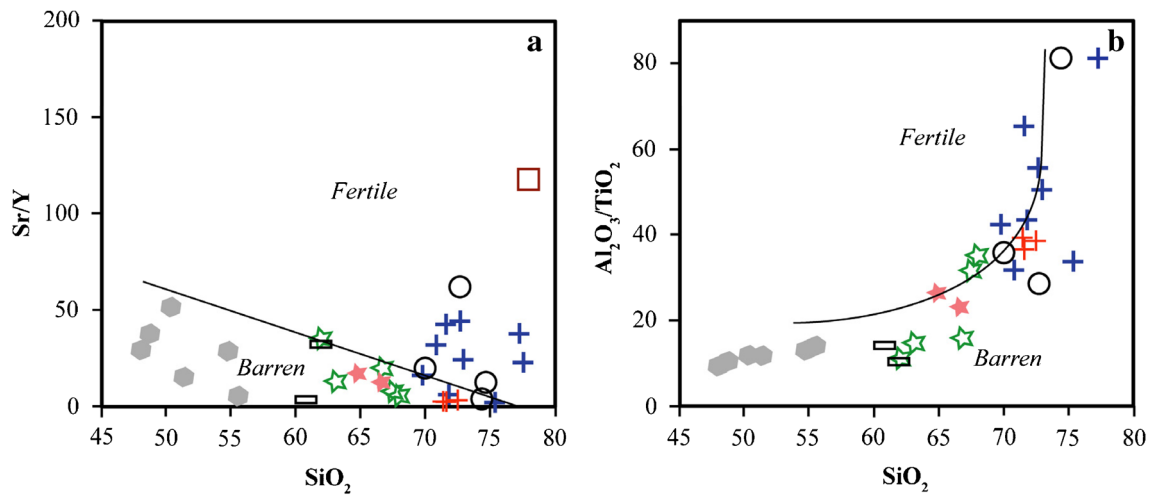


**Fig. 6** Plot of whole rock chemistry of the Mbengwi granitoids on discriminating diagrams of Loucks (2014). **a** Sr/Y vs. SiO<sub>2</sub> (wt.%) diagram. **b** Al<sub>2</sub>O<sub>3</sub>/TiO<sub>2</sub> vs. SiO<sub>2</sub> (wt.%)

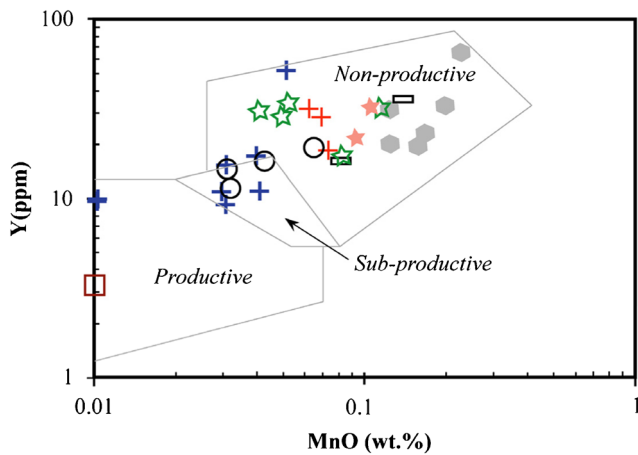


**Fig. 7** Whole rock Y vs. MnO diagram of Baldwin and Pearce (1982) for the Mbengwi granitoids

and 8, respectively. The projection of the studied plutonics in the A/CNK vs. A/NK diagram (Fig. 2a) reveals that compositions of some granitoids are essentially comparable to calc-alkaline granitoids associated with Cu, Zn, W, and Mo skarn. Monzodiorites and few intermediate rocks (monzonites, one Qtz-monzonite, and a granodiorite sample) overlap Fe and Cu skarn granitoids fields. In the (Na<sub>2</sub>O + K<sub>2</sub>O) versus SiO<sub>2</sub> diagram, the intermediate phases of the Mbengwi granitic rocks remain close to Zn and Cu skarn-related granitoids (Fig. 8a). Plotting of the studied rocks in the AFM diagram reveals that their compositions seem to be similar to those of granitoids associated with all skarn types (Fig. 8b), although this diagram indicates that compositions of the intermediate phases are alike to magmatic districts related to Zn and Cu mineralization. Using the Nb versus Y and Rb versus (Y + Nb) discriminative diagrams, the compositions of the Mbengwi granitoids

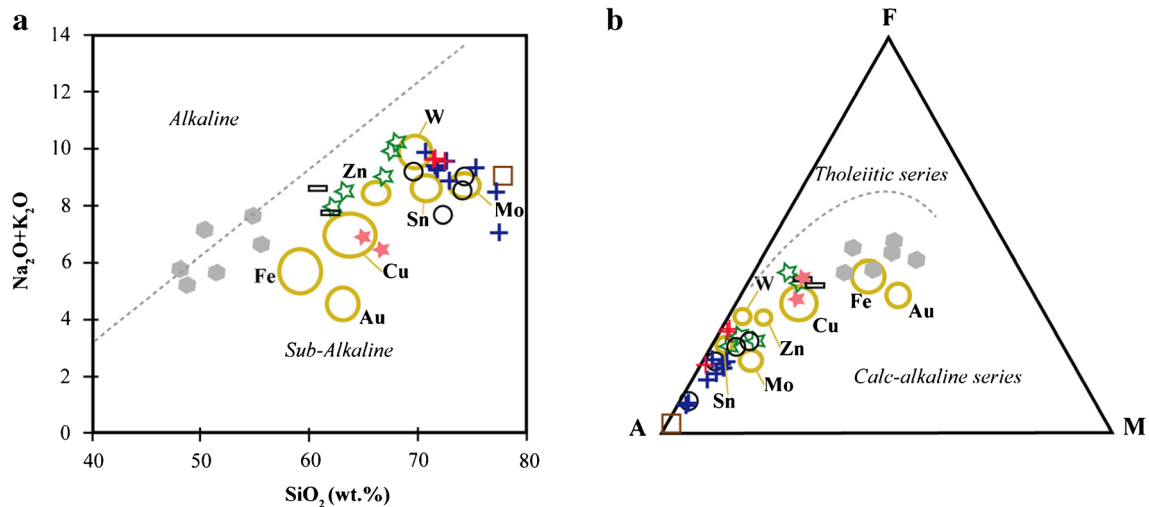


**Fig. 8** Plotting of the Mbengwi granitoids composition together with the mean composition of various mineralized granitoids with related metals (of which the names are indicated) are from Meinert (1995) in **a** K<sub>2</sub>O +

Na<sub>2</sub>O (wt.%) vs. SiO<sub>2</sub> (wt.%) of Rickwood (1989) and **b** AFM diagram of Irvine & Baragar (1971)

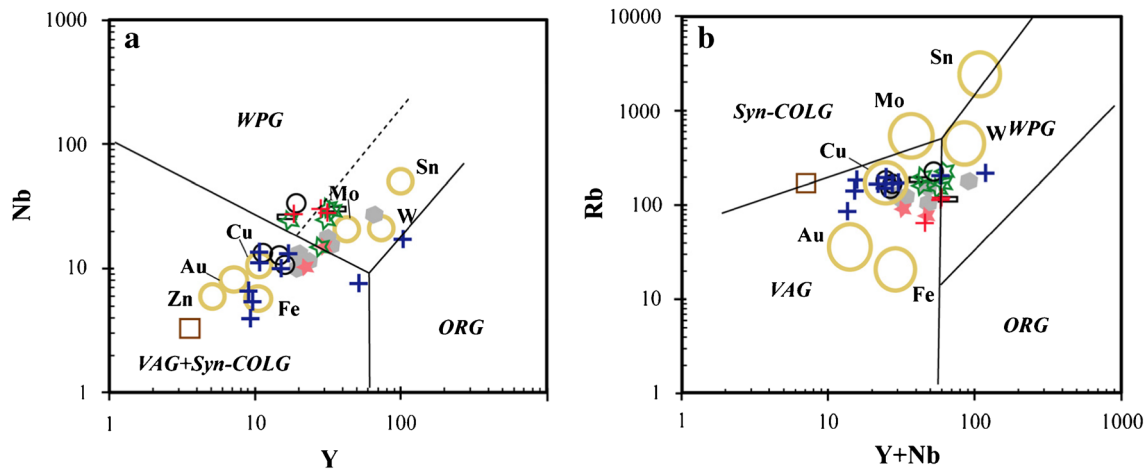


**Fig.9** a, b Nb vs. Y and Rb vs. (Y+Nb) diagrams (Pearce et al. 1984; see also Förster et al. 1997); ORG = ocean-ridge granites; syn-COLG = syncollisional granites; VAG = volcanic arc granites; WPG = within-plate granites

plot nearby Cu, Fe, Au, Mo, W, and Zn skarn-related granitoids (Fig. 9). However, it should be noticed that samples plotting within the skarn-related granitoids domain in Fig. 2 are not necessarily the same exhibiting high contents in Cu, Pb, Th, and Zn. The most widespread skarn mineral observed in the studied sample is pyrite (not analyzed). This mineral occurs as disseminated small grains.

**Thorium mineralization**

Th mineralization occurs in the upper continental crust, particularly in placers, granitic rocks, or veins. The determination of the Th mineralizing potential and consequently the discrimination between unproductive and mineralized granitic rocks from Mbengwi was based on the analysis of their contents in P, followed by the use of the  $P_2O_5 * 100/Th$  vs. B (B = Ti + Fe + Mg) diagram in accordance with Scheepers (2000).

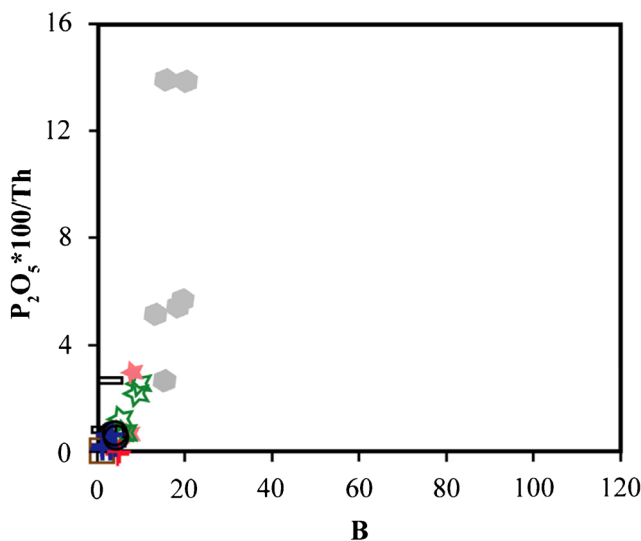


**Fig. 10** Plots  $P_2O_5 * 100/Th$  versus B (B = Ti + Fe + Mg) for the Mbengwi granitoids

According to the previous author, Th-mineralized granitic rocks are particularly enriched in P/Th and their composition trend in the  $P_2O_5 * 100/Th$  vs. B diagram is nearly parallel to the Y axis. The use of this diagram for the studied granitic rocks (Fig. 10) reveals that the general trend is almost vertical and that monzodiorites and monzonites are almost parallel to the Y axis and can therefore be considered as mineralized or potentially mineralized.

**Conclusions**

The calc-alkaline affinity alongside the I-type nature and the range of Sr/Y ratios of the Mbengwi granitoids evidence that their parental magmas particularly those of granites are likely fertile for Cu mineralization, related skarn, and for some metals, epithermal deposits. Nevertheless, they have not experienced post-magmatic hydrothermal activity required for Sn, U, W, or Ta mineralization, given that they are moderately differentiated and have high K/Rb ratios.

Several geochemical criteria such as color index, Rb/Sr, Ce/Yb, Sm/Eu, or Rb/Ba ratios in addition to the behavior of Rb, Ba, and Sr disclose the barren nature of the Mbengwi granitoids regarding Sn, and Mo; though they might be rather productive concerning Cu and mainly fertile regarding Zn, although we have not yet really observed minerals bearing those elements.

**Acknowledgements** We are thankful to the French Ministry of Foreign Affairs for the three stays of a total duration of 12 months, awarded to BJ Mbassa, as part of a doctoral scholarship in France, EGIDE and GET-UMR 5563-CNRS for accommodation and analytical facilities. The co-authors also wish to dedicate this work to Junior Désiré Nolla, who died after a short illness on July 20, 2017. We mourn the loss of a human being of both exceptional qualities and a promising colleague. We are grateful to anonymous reviewer and the Editor-in-Chief Abdullah M. Al-Amri for the constructive reviews and insightful comments.

## References

- Ahmadian J, Sarjoughian F, Lentz D, Esna-Ashari A, Murata M, Ozawa H (2015) Eocene K-rich adakitic rocks in the Central Iran: implications for evaluating its Cu–Au–Mo metallogenic potential. *Ore Geol Rev* 72:323–342
- Aries S, Valladon M, Polvé M, Dupré B (2000) A routine method for oxide and hydroxide interference corrections in ICP-MS chemical analyses of environmental and geological samples. *Geostand Newslett* 24:19–31
- Asadi A, Moore F, Zarasvandi A (2014) Discriminating productive and barren porphyry copper deposits in the southeastern part of the central Iranian volcano-plutonic belt, Kerman region, Iran: a review. *Earth-Sci Rev* 138:25–46
- Bahajroy M, Taki S (2014) Study of the mineralization potential of the intrusives around Valis (Tarom-Iran). *Earth Sci Res J* 18:123–129
- Baldwin JA, Pearce JA (1982) Discrimination of productive and non-productive porphyritic intrusions in the Chilean Andes. *Econ Geol* 77:664–674
- Bea F, Fershtater G, Corretge LG (1992) The geochemistry of P in granitic rocks and the effect of aluminium. *Lithos* 29:43–56
- Bea F, Montero P, Ortega M (2006) A LA-ICP-MS evaluation of Zr reservoirs in common crustal rocks: implications for Zr and Hf geochemistry, and zircon forming processes. *Can Mineral* 44:693–714
- Benoit M, Polvé M, Ceuleneer G (1996) Trace element and isotopic characterization of mafic cumulates in a fossil mantle diaper (Oman ophiolite). *Chem Geol* 134:199–214
- Blevin P (2003) Metallogeny of granitic rocks. In: Magmas to mineralization. Blevin P et al. (eds). The Ishihara symp, pp 1–4
- Djouka-Fonkwé ML, Schulz B, Schüssler U, Tchouankoué J-P, Nzolang C (2008) Geochemistry of the Bafoussam Pan–African I- and S-type granitoids in western Cameroon. *J Afr Earth Sci* 50:148–167
- Dumort JC (1968) Carte géologique de reconnaissance du Cameroun à l'échelle du 1/500000, coupe Douala-Ouest avec notice explicative. Bulletin de la direction de géologie et des mines, Cameroun
- Eugster HP (1985) Granites and hydrothermal ore deposits: a geochemical framework. *Mineral Mag* 49:7–23
- Förster HJ, Tischendorf G, Trumbull RB (1997) An evaluation of the Rb vs. (Y+Nb) discrimination diagram to infer tectonic setting of silicic igneous rocks. *Lithos* 40:261–293
- Gao Y, Santosh M, Wei R, Ma G, Chen Z, Wu J (2013) Origin of high Sr/Y magmas from the northern Taihang Mountains: implications for Mesozoic porphyry copper mineralization in the North China Craton. *J Asian Earth Sci* 78:143–159
- Ghods MR, Boomeri M, Bagheri S, Lentz D, Ishiyama D (2016) Metallogeny and mineralization potential of the Bazman Granitoids, SE Iran. *Resour Geol* 66(3):286–302
- Govett GJS, Atherden PR (1988) Application of rock geochemistry to productive plutons and volcanic sequences. *Geochem Explor* 30:223–242
- Hou Z, Zhang H, Pan X, Yang Z (2011) Porphyry Cu (–Mo–Au) deposits related to melting of thickened mafic lower crust: examples from the eastern Tethyan metallogenic domains. *Ore Geol Rev* 3:21–45
- Irvine TN, Baragar WRA (1971) A guide to the chemical classification of the common volcanic rocks. *Can J Earth Sci* 8:523–548
- Karimpour MH (1999) Application of Sm/Eu, Rb/Sr, Ce/Yb and F/Rb ratios to discriminate between tin mineralized and non-mineralized S-type granite. *J Geosci* 7:1–16
- Karimpour MH, Bowes WW (1983) Application of trace elements and isotopes for discriminating between porphyry molybdenum, copper, and tin systems and the implications for predicting the grade. *Glob Tecton Metallogen* 2:1–16
- Kwékam M, Liégeois J-P, Njonfang E, Affaton P, Hartmann G, Tchoua MF (2010) Nature, origin and significance of the Fomopéa Pan–African high–K calc–alkaline plutonic complex in the Central African fold belt (Cameroon). *J Afr Earth Sci* 57:79–95
- Kwékam M, Affaton P, Bruguier O, Liégeois J-P, Hartmann G, Njonfang E (2013) The Pan-African Kekem gabbro-norite (West-Cameroon), U–Pb zircon age, geochemistry and Sr–Nd isotopes: Geodynamical implication for the evolution of the Central African fold belt. *J Afr Earth Sci* 84:70–88
- Lehmann B, Mahawat C (1989) Metallogeny of tin in Central Thailand: a genetic concept. *Geology* 17:426–429
- Lentz DR (1998) Petrogenetic and geodynamic implications of extensional regimes in the Phanerozoic subduction zones and their relationship to VMS-forming systems. *Ore Geol Rev* 12:289–327
- Loucks RR (2014) Distinctive composition of copper-ore forming arc magmas. *Aust J Earth Sci* 61:5–16
- Maniar PD, Piccoli PM (1989) Tectonic discrimination of granitoids. *Geol Soc Am Bull* 101:635–643
- Mbassa BJ (2015) Petrographic, mineralogical, geochemical and geochronological characterizations of the magmatic formations from Mbengwi (NW–Cameroon, central Africa). Ph.D thesis, Univ Yaoundé I
- Mbassa BJ, Njonfang E, Benoit M, Grégoire M, Kamgang P, Duchene S, Brunet P, Ateba B, Tchoua MF (2012) Mineralogy, geochemistry and petrogenesis of the recent magmatic formations from Mbengwi, a continental sector of the Cameroon Volcanic Line (CVL), Central Africa. *Mineral Petrol* 106:217–242
- Mbassa BJ, Kamgang P, Grégoire M, Njonfang E, Benoit M, Itiga Z, Duchene S, Bessong M, Wonkwenmendiam NP, Ntepe N (2016) Evidence of heterogeneous crustal origin for the Pan-African Mbengwi granitoids and the associated mafic intrusions (northwestern Cameroon, Central Africa). *Compt Rendus Geosci* 348:116–126
- McDonough WF, Sun SS (1995) The composition of the Earth. *Chem Geol* 120:223–253
- Meinert LD (1995) Compositional variation of igneous rocks associated with skarn deposits – Chemical evidence for a genetic connection between petrogenesis and mineralization. In: Thompson JFH (ed) Magmas fluids and ore deposits, Min Assoc Can Short Course Series 23:401–418
- Milesi JP, Toteu SF, Deschamps Y, Feybessé JL, Lerouge C et al (2006) An overview of the geology and major ore deposits of Central Africa: Explanatory note for the 1:4,000,000 map “Geology and major ore deposits of Central Africa”. *J Afr Earth Sci* 44:571–595
- Nédélec A, Bouchez JL (2011) Pétrologie des granites, structure, cadre géologique. Collect Interact, Vuibert
- Neiva AMR, Silva MMVG, Gomes MEP, Campos TFC (2002) Geochemistry of coexisting biotite and muscovite of Portuguese peraluminous granitic differentiation series. *Chem Erde* 62:197–215
- Njanko T, Nédélec A, Affaton P (2006) Synkinematic high-K calc-alkaline plutons associated with the Pan-African Central Cameroon shear zone (W-Tibati area): petrology and geodynamic significance. *J Afr Earth Sci* 44:494–510
- Nzenti JP, Kapajika B, Wömer G, Lubala TR (2006) Synkinematic emplacement of granitoids in a Pan-African shear zone in Central Cameroon. *J Afr Earth Sci* 45:74–86
- Nzolang C, Kagami H, Nzenti J-P, Holtz F (2003) Geochemistry and preliminary Sr–Nd isotopic data on the Neoproterozoic granitoids from the Bantoum area, West Cameroon. Evidence for a derivation from a Paleoproterozoic to Archean crust. *Polar Geosci* 16:196–226
- Pearce JA, Harris NBW, Tindle AG (1984) Trace element discrimination diagrams for the tectonic interpretation of granitic rocks. *J Petrol* 25:956–983
- Pei R, Hong D (1995) The granites of South China and their metallogeny. *Episodes* 18:77–82
- Peron Y (1969) Notice explicative sur la feuille Wum-Banyo avec carte géologique de reconnaissance au 1/500.000, Direction des Mines et de la Géologie. Yaoundé, Cameroun

- Richards JP (2011) Magmatic to hydrothermal meta flux in convergent and collided magins. *Ore Geol Rev* 40:1–26
- Richards JP, Spell T, Rameh E, Razique A, Fletcher T (2012) High Sr/Y magmas reflect arc maturity, high magmatic water content, and porphyry Cu ± Mo ± Au potential: examples from the Tethyan Arcs of Central and Eastern Iran and western Pakistan. *Econ Geol* 107:295–332
- Rickwood PC (1989) Boundary lines within petrologic diagrams which use oxides of major and minor elements. *Lithos* 22:247–263
- Rossi JN, Toselli AJ, Basei MA, Sial AN, Baez M (2011) Geochemical indicators of metalliferous fertility in the Carboniferous San Blas pluton, Sierra de Velasco, Argentina. In: Sial AN et al (eds) *Granite-Related Ore Deposits*. *Geol Soc Vol*, vol 350. *Spec Pub*, London, pp 175–186
- Rozendaal A, Bruwer L (1995) Tourmaline nodules: mineralization in the Cape Granite Suite, South Africa. *J Afr Earth Sci* 21:141–155
- Ruiz C, Fernández-Leyva CF, Locutura J (2008) Geochemistry, geochronology and mineralization potential of the granites in the Central Iberian Zone: the Jalama batholith. *Chem Erde* 68:413–429
- Scheepers R (2000) Granites of the Saldania mobile belt, South Africa: radioelements and P as discriminators applied to metallogeny. *J Geochem Explor* 68:69–86
- Shafiei B, Haschke M, Shahabpour J (2009) Recycling of orogenic arc crust triggers porphyry Cu mineralization in Kerman Cenozoic arc rocks, southeastern Iran. *Mineral Deposita* 44:265–283
- Sillitoe RH (1996) Granites and metal deposits. *Episodes* 19:126–133
- Sillitoe RH (2010) Porphyry copper systems. *Econ Geol* 105:3–41
- Spinks SC, Uvarova Y, Thorne R, Anand R, Reid N, White A, Ley-Cooper Y, Bardwell N, Gray D, Meadows H, LeGras M (2017) Detection of zinc deposits using terrestrial ferromanganese crusts. *Ore Geol Rev* 80:484–503
- Tchameni R, Pouclet A, Penaye J, Ganwa AA, Toteu SF (2006) Petrography and geochemistry of the Ngaoundéré Pan-African granitoids in central North Cameroon: implications for their sources and geological setting. *J Afr Earth Sci* 44:543–560
- Wedepohl KH (1995) The composition of the continental crust. *Geochim Cosmochim Acta* 59:1217–1232
- Weis D, Frey FA (1991) Isotope geochemistry of the Ninetyeast Ridge basement basalts: Sr, Nd, and Pb evidence for involvement of the Kerguelen hot spot. *Proc Ocean Drill Program Sci Results* 121:591–610
- Wolfe WJ (1977) Geochemical exploration of early Precambrian volcanogenic sulphide mineralization in Ben Nevis Township, District of Cochrane: Ontario. *Geol Survey Study* 19:39
- Wu S, Zheng Y, Sun X (2016) Subduction metasomatism and collision-related metamorphic dehydration controls on the fertility of porphyry copper ore-forming high Sr/Y magma in Tibet. *Ore Geol Rev* 73: 83–103
- Zarasvandi A, Rezaei M, Sadeghi M, Lentz D, Adelpour M, Pourkaseb H (2015) Rare earth element signatures of economic and sub-economic porphyry copper system in Urumieh-Dokhtar Magmatic Arc (UDMA), Iran. *Ore Geol Rev* 70:407–423